Journal of Engineering Mathematics **28**: 145–171, 1994.
© 1994 *Kluwer Academic Publishers. Printed in the Netherlands.*

Free-convection stagnation-point boundary layers driven by catalytic surface reactions: I the steady states

M.A. CHAUDHARY and J.H. MERKIN
Department of Applied Mathematics, University of Leeds, Leeds LS2 9JT, U.K.

Received 28 October 1992; accepted in revised form 19 July 1993

Abstract. The free convection boundary-layer flow near a stagnation point driven by catalytic surface heating is considered. The case without fuel consumption is treated first, and it is shown that the steady state equations admit multiple solutions. Explicit expressions can be obtained for these solution branches and it is found that a hysteresis point occurs when the activation energy parameter $\varepsilon = 1/5$. The effect of fuel consumption is seen to be characterised by the dimensionless parameter α and numerical results are obtained for a range of values of α and ε, as well as Prandtl number σ and Schmidt number S_c. Multiple solutions are again observed and analytic expressions for the bifurcation points can be found when $\sigma = S_c$. For $\sigma \neq S_c$ these have to be determined numerically.

1. Introduction

Many chemically reacting systems involve both homogeneous and heterogeneous reactions, with examples occurring in combustion, catalysis and biochemical systems. The interaction between the homogeneous reactions in the bulk of the fluid and the heterogeneous reactions occurring on some catalytic surface is generally very complex, involving the production and consumption of reactant species at different rates both within the fluid and on the catalytic surface as well as the feedback on these reaction rates through temperature variations within the reacting fluid, which in turn modify the fluid motion. Thus there is a three-way coupling between fluid flow, fluid/surface temperatures, and reactant species concentrations.

Previous studies of this problem have assumed that the whole of the reaction occurs within a boundary-layer region on the catalytic surface and have assumed that the heat transfer is by forced convention, with an outer flow being prescribed at the edge of the boundary layer region, the interaction between the fluid flow and heat transfer then being achieved via the temperature dependence of the fluid properties. Two flow configurations have been treated, namely a stagnation point flow and flow over a flat plate. The former case was treated originally by Chambre [1] and extended later by Law [2], Ablow et al. [3], and Trevino [4], with detailed studies of extinction and ignition criteria being undertaken by Giovangigli and Candel [5] and Song et al. [6]. The bifurcation behaviour of the steady states has been treated by Song et al. [7]. This stagnation point model has been applied to strained premixed flames by Law and Sivashinsky [8] and Libby and Williams [9]. The equivalent problem for the boundary-layer flow over a flat plate has been discussed by Trevino and Fernandez-Pello [10] who used the basic Blasius solution for the flow. The conditions for ignition and extinction for this flow were considered by Linan and Trevino [11] and Fakheri and Buckius [12]. A numerical solution of the boundary-layer equations for this problem has been presented by Chen and Tien [13].

It is clear from the experimental work on homogeneous-heterogeneous reactions that large temperature differences can be generated within the boundary layer on the catalytic surface,

see, for example, Williams et al. [14]. These temperature differences can set up substantial buoyancy-driven secondary flows within the boundary layer and thus can greatly modify the basic forced-convection heat transfer mechanism. In some situations free convection could be the dominant heat transfer process, and it is this aspect that we examine in the present paper.

To this end we consider a much simplified model of this complex problem, isolating the free convection aspect and the catalytic surface reaction. In particular, we assume that the flow in the boundary layer is driven purely by free convection and consider only heterogeneous reactions, i.e., we assume that reaction takes place only on the catalytic surface. We consider the stagnation point flow configuration and, for simplicity, we make the standard Boussinesq approximation, taking fluid properties and fluid density to be constant (except in the buoyancy force). The purpose of the present study is then to isolate just one part of the full homogeneous-heterogeneous reaction problem and examine this particular aspect in detail. The simplicity of our model enables us to determine many of the important features analytically, but, perhaps more importantly, it enables us to identify clearly the basic mechanisms involved. The inclusion of further effects, such as homogeneous reactions and forced flow, can then be assessed against this basic solution. These additional features will be treated in subsequent papers.

We start by considering the case of no fuel consumption. We find ranges of parameter values for which there are multiple solutions of the steady state equations. We are able to give explicit expressions for these, from which we are able to deduce that a hysteresis point (change from multiple to single solutions) occurs at $\varepsilon = 1/5$, where ε is the usual activation energy parameter. When we allow for fuel consumption, we still find ranges of parameter values over which there are multiple solutions. However, now the upper solution branch corresponds to much lower surface temperatures. We are able to give explicit expressions for hysteresis points and the limiting behaviour on the upper branch when the Schmidt number S_c and Prandtl number σ are equal. For $S_c \neq \sigma$ we find that these values have to be determined by numerical calculations.

2. Equations

We consider a catalytic body surrounded by a fluid at rest and at a constant temperature T_0. We assume that on the surface of the catalyst, the single, first order, exothermic reaction governed by Arrhenius kinetics

$$A \rightarrow B\,, \qquad \text{rate} = k_0 a\, \mathrm{e}^{-E/RT}$$

takes place where B is the product species, k_0 is a constant, E is the activation energy and R is the gas constant. We also assume that no further reaction takes place in bulk of the fluid and that well away from the surface the concentration of the reactant A is uniform at a value a_0. Heat is released by the reaction at rate $Qk_0 a\, \mathrm{e}^{-E/RT}$ where Q is heat of reaction. This heat is taken from the body surface into the surrounding fluid by conduction and thus a natural convection flow is set up.

We take the Grashof number of this convective flow to be larger enabling us to make the usual boundary-layer simplification. We further make use of Boussinesq approximation, i.e., we neglect changes in density except in the body force (buoyancy) and assume that the fluid properties remain constant.

The governing equations for this (two-dimensional) flow are

$$\frac{\partial u}{\partial x}+\frac{\partial v}{\partial y}=0\,, \tag{1a}$$

$$\frac{\partial u}{\partial t}+u\frac{\partial u}{\partial x}+v\frac{\partial u}{\partial y}=g\beta(T-T_0)S(x)+\nu\frac{\partial^2 u}{\partial y^2}\,, \tag{1b}$$

$$\frac{\partial T}{\partial t}+u\frac{\partial T}{\partial x}+v\frac{\partial T}{\partial y}=\frac{\nu}{\sigma}\frac{\partial^2 T}{\partial y^2}\,, \tag{1c}$$

$$\frac{\partial a}{\partial t}+u\frac{\partial a}{\partial x}+v\frac{\partial a}{\partial y}=\frac{\nu}{S_c}\frac{\partial^2 a}{\partial y^2}\,, \tag{1d}$$

x and y are the co-ordinates measuring distance along and normal to the body surface, with corresponding velocity components u and v. T and a are the temperature and concentration respectively of the reactant A within the boundary-layer. β is the coefficient of thermal expansion, σ is Prandtl number, ν is kinematic viscosity, S_c is Schmidt number and $S(x)=\sin\phi$ where ϕ is the angle between the outward normal and downward vertical direction.

The initial and boundary conditions are

$$u=v=0\,,\qquad a=a_0\,,\qquad T=T_0\quad \text{at } t=0\,, \tag{2a}$$

$$u\to 0\,,\qquad a\to a_0\,,\qquad T\to T_0\quad \text{as } y\to\infty\,, \tag{2b}$$

$$u=v=0\,,\qquad k_c\left(\frac{\partial T}{\partial y}\right)=-Qk_0 a\,\mathrm{e}^{-E/RT}\,,\qquad D\left(\frac{\partial a}{\partial y}\right)=k_0 a\,\mathrm{e}^{-E/RT}\,,\quad \text{on } y=0\,, \tag{2c}$$

where k_c and D are thermal conductivity and mass diffusivity respectively.

To make Eqs (1) and (2) dimensionless we use the standard (Frank–Kamenetskii) variable for the temperature, namely $T-T_0=RT_0^2\theta/E$. This gives a temperature scale $T_s=RT_0^2/E$ and leads to a velocity scale $U_s=(g\beta T_s l)^{1/2}=(g\beta l(RT_0^2/E))^{1/2}$ and Grashof number $G_r=g\beta T_s l^3/\nu^2=g\beta l^3 RT_0^2/E\nu^2$ where l is a length scale for the body.

We then introduce the further dimensionless variables as

$$\bar{x}=\frac{x}{l}\,,\qquad \bar{y}=\frac{y}{l}G_r^{1/4}\,,\qquad \bar{t}=\frac{U_s}{l}t\,,\qquad \bar{a}=\frac{a}{a_0}\,,\qquad u=U_s\bar{u}\,,\qquad v=U_s G_r^{-1/4}\bar{v}\,, \tag{3}$$

so that Eqs (1) take the form

$$\frac{\partial\bar{u}}{\partial\bar{x}}+\frac{\partial\bar{v}}{\partial\bar{y}}=0\,, \tag{4a}$$

$$\frac{\partial\bar{u}}{\partial\bar{t}}+\bar{u}\frac{\partial\bar{u}}{\partial\bar{x}}+\bar{v}\frac{\partial\bar{u}}{\partial\bar{y}}=\theta S(\bar{x})+\frac{\partial^2\bar{u}}{\partial\bar{y}^2}\,, \tag{4b}$$

$$\frac{\partial\theta}{\partial\bar{t}}+\bar{u}\frac{\partial\theta}{\partial\bar{x}}+\bar{v}\frac{\partial\theta}{\partial\bar{y}}=\frac{1}{\sigma}\frac{\partial^2\theta}{\partial\bar{y}^2}\,, \tag{4c}$$

$$\frac{\partial \bar{a}}{\partial \bar{t}} + \bar{u}\frac{\partial \bar{a}}{\partial \bar{x}} + \bar{v}\frac{\partial \bar{a}}{\partial \bar{y}} = \frac{1}{S_c}\frac{\partial^2 \bar{a}}{\partial \bar{y}^2}. \tag{4d}$$

The initial and boundary conditions (2) become

$$\bar{u} = \bar{v} = 0, \quad \theta = 0, \quad \bar{a} = 1 \quad \text{at } \bar{t} = 0, \tag{5a}$$

$$\bar{u} \to 0, \quad \theta \to 0, \quad \bar{a} \to 1 \quad \text{as } \bar{y} \to \infty, \tag{5b}$$

$$\bar{u} = \bar{v} = 0, \quad \frac{\partial \theta}{\partial \bar{y}} = -\lambda \bar{a}\, e^{\theta/1+\varepsilon\theta}, \quad \frac{\partial \bar{a}}{\partial \bar{y}} = \alpha\lambda \bar{a}\, e^{\theta/1+\varepsilon\theta} \quad \text{on } \bar{y} = 0, \tag{5c}$$

where $\varepsilon = RT_0/E$ and the dimensionless parameters λ and α are given by

$$\lambda = \frac{EQk_0 l a_0\, e^{-E/RT_0}}{G_r^{1/4} k_c RT_0^2}, \qquad \alpha = \frac{k_c RT_0^2}{a_0 QED}.$$

The problem defined by Eqs (4) and (5) requires the solution of the full time-dependent boundary-layer equations. However, a simplification can be made, and clear insight into the nature of the general problem be obtained, if we consider the flow near a forward stagnation point.

In this case $S(x) = x$ and we then put

$$\psi = xf(y, t), \quad \theta = \theta(y, t), \quad a = a(y, t), \tag{6}$$

where ψ is the stream function, defined in the usual way, and where we have dropped the bars for convenience. This leads to the reduced system of equations

$$\frac{\partial^3 f}{\partial y^3} + f\frac{\partial^2 f}{\partial y^2} - \left(\frac{\partial f}{\partial y}\right)^2 + \theta = \frac{\partial^2 f}{\partial y\, \partial t}, \tag{7a}$$

$$\frac{1}{\sigma}\frac{\partial^2 \theta}{\partial y^2} + f\frac{\partial \theta}{\partial y} = \frac{\partial \theta}{\partial t}, \tag{7b}$$

$$\frac{1}{S_c}\frac{\partial^2 a}{\partial y^2} + f\frac{\partial a}{\partial y} = \frac{\partial a}{\partial t}, \tag{7c}$$

with the same initial boundary conditions as before.

As is usual in combustion problems, a necessary pre-requisite to understanding the full time-dependent problem is a discussion of the possible steady states. This leads us to consider the similarity system

$$f''' + \theta + ff'' - f'^2 = 0, \tag{8a}$$

$$\frac{1}{\sigma}\theta'' + f\theta' = 0, \tag{8b}$$

$$\frac{1}{S_c}a'' + fa' = 0, \tag{8c}$$

subject to the boundary conditions

$$f = f' = 0\,, \qquad \theta' = -\lambda a\, e^{\theta/1+\varepsilon\theta}\,, \qquad a' = \alpha\lambda a\, e^{\theta/1+\varepsilon\theta} \quad \text{on } y = 0\,, \tag{9a}$$

$$f' \to 0\,, \qquad \theta \to 0\,, \qquad a \to 1 \quad \text{as } y \to \infty\,, \tag{9b}$$

where primes denote differentiation with respect to y.

A common starting point for the discussion of combustion problems is to examine their behaviour when the effects of reactant consumption are ignored. A discussion of this reduced model then enables some of the basic features of the full model to be identified more easily and also provides a framework against which to discuss the full model. This is where we start our discussion.

3. Non fuel consumption case ($\alpha = 0$)

With $\alpha = 0$, $a \equiv 1$ and Eqs (8) and (9) reduce to

$$f''' + \theta + ff'' - f'^2 = 0\,, \tag{10a}$$

$$\frac{1}{\sigma}\theta'' + f\theta' = 0\,, \tag{10b}$$

subject to

$$f = 0\,, \qquad f' = 0\,, \qquad \theta' = -\lambda\, e^{\theta/(1+\varepsilon\theta)} \quad \text{on } y = 0\,, \tag{11a}$$

$$f' \to 0\,, \qquad \theta \to 0 \quad \text{as } y \to \infty\,. \tag{11b}$$

Equations (10) and (11) were solved numerically using a standard two-point boundary-value problem solver. To do this and to allow for the possibility of multiple solutions we specified the value of $\theta(0)$ and used λ as one of the parameters to be determined. The results for typical cases, shown by plots of $\theta(0)$ against λ, are given in Fig. 1 (for $\varepsilon = 0$) and Fig. 2 (for

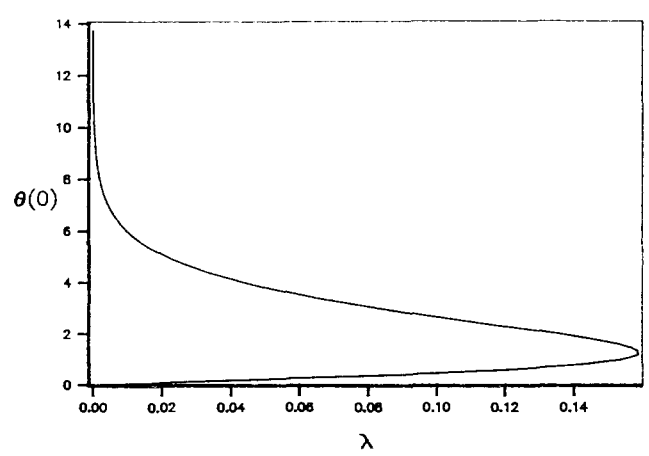

Fig. 1. Graph of $\theta(0)$ against λ obtained from the numerical solution of Eqs (10) and (11) for $\varepsilon = 0$ and $\sigma = 1$.

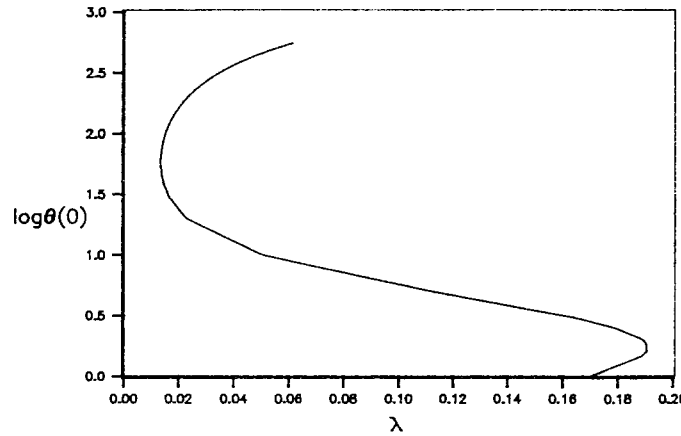

Fig. 2. Graph of $\log\theta(0)$ against λ obtained from the numerical solution of Eqs (10) and (11) for $\varepsilon = 0.1$ and $\sigma = 1.0$.

$\varepsilon = 0.1$). In both cases we took $\sigma = 1.0$. (Note that in order to show both turning points for the $\varepsilon = 0.1$ case we have plotted $\log\theta(0)$ against λ in Fig. 2, the behaviour of $\theta(0)$ for λ small on the lower branch is similar to that shown in Fig. 1.)

An important feature of both of these graphs is the existence of critical (or turning) points. These represent a change in stability of the steady state (through a saddle-node bifurcation) and limit the range of existence of solution. There is also the further possibility of the existence of a hysteresis point at a sufficiently large value of ε, ε_H (say), with the dependence of $\theta(0)$ on λ then being monotone for $\varepsilon > \varepsilon_H$. It is this aspect that we now discuss.

To calculate the critical points λ_c as they vary with ε (and σ), we put

$$\lambda = \lambda_c - \delta\,, \qquad 0 < |\delta| \ll 1\,.$$

Due to the parabolic nature of curve near λ_c, we expand

$$\left.\begin{aligned} f &= f_0 + |\delta|^{1/2} f_1 + \cdots \\ \theta &= \theta_0 + |\delta|^{1/2}\theta_1 + \cdots \end{aligned}\right\}, \tag{12}$$

The leading order equations are

$$\left.\begin{aligned} &f_0''' + \theta_0 + f_0 f_0'' - f_0'^2 = 0 \\ &\frac{1}{\sigma}\theta_0'' + f_0\theta_0' = 0 \end{aligned}\right\}, \tag{13}$$

with boundary conditions

$$f_0(0) = f_0'(0) = 0\,; \qquad \theta_0'(0) = -\lambda_c \exp\left(\frac{\theta_0}{1+\varepsilon\theta_0}\right) \quad \text{on } y = 0\,, \tag{14a}$$

$$f_0' \to 0\,, \qquad \theta_0 \to 0 \quad \text{as } y \to \infty\,. \tag{14b}$$

The equations at $O(|\delta^{1/2}|)$ are

$$f_1''' + \theta_1 + f_0 f_1'' + f_0'' f_1 - 2f_0' f_1' = 0\,, \tag{15a}$$

$$\frac{1}{\sigma}\theta_1'' + f_0\theta_1' + f_1\theta_0' = 0\,, \tag{15b}$$

subject to the boundary conditions

$$f_1(0) = f_1'(0) = 0\,, \qquad \theta_1'(0) = -\lambda_c \exp\left(\frac{\theta_0}{1+\varepsilon\theta_0}\right)\frac{\theta_1}{(1+\varepsilon\theta_0)^2} \quad \text{on } y = 0\,, \tag{16a}$$

$$f_1' \to 0\,, \qquad \theta_1 \to 0 \quad \text{as } y \to \infty\,. \tag{16b}$$

The equations (15) together with boundary conditions (16) form a homogeneous problem which has, in general, only a trivial solution. However, it is the existence of a non-trivial solution (forced by taking $\theta_1(0) = 1$ (say)) which gives the value of λ_c.

Now suppose that problem formed by the leading order equations has a solution (θ_0^c, f_0^c) with $\theta_0^c(0) = b_0$ so that

$$\frac{\partial\theta_0^c}{\partial y} = -\lambda_c \exp\left(\frac{b_0}{1+\varepsilon b_0}\right) \quad \text{on } y = 0\,, \tag{17a}$$

However, Eqs (15) have the solution

$$\begin{aligned} f_1 &= K\left(y\frac{\mathrm{d}f_0^c}{\mathrm{d}y} + f_0^c\right), \\ \theta_1 &= K\left(y\frac{\mathrm{d}\theta_0^c}{\mathrm{d}y} + 4\theta_0^c\right), \end{aligned} \tag{17b}$$

for some constant K and for all values of σ. (This solution also satisfies the boundary conditions $f_1(0) = f_1'(0) = 0$, $f_1'(\infty) = \theta_1(\infty) = 0$.)

The non-trivial condition $(\theta_1(0) = 1)$ and the boundary condition

$$\theta_1'(0) = -\lambda_c \frac{\exp\left(\dfrac{b_0}{1+\varepsilon b_0}\right)}{(1+\varepsilon b_0)^2}\,,$$

are satisfied provided $K = 1/4b_0$ and, using (17a),

$$5K\left(\frac{\mathrm{d}\theta_0^c}{\mathrm{d}y}\right)_0 = -\lambda_c \frac{\exp\left(\dfrac{b_0}{1+\varepsilon b_0}\right)}{(1+\varepsilon b_0)^2} = -5K\lambda_c \exp\left(\frac{b_0}{1+\varepsilon b_0}\right), \tag{18a}$$

(18a) gives

$$\frac{5}{4b_0}(1+\varepsilon b_0)^2 = 1\,.$$

which leads to a quadratic equation for b_0 with solution

$$b_0 = \frac{(2-5\varepsilon) \pm 2\sqrt{1-5\varepsilon}}{5\varepsilon^2}\,. \tag{18b}$$

Equation (18b) gives two values of b_0 provided $\varepsilon < 1/5$ and we get a hysteresis point at $\varepsilon_H = 1/5$ (with $b_0 = 5$).

Note that as $\varepsilon \to 0$ the two solutions behave like

$$\left.\begin{aligned} b_0 &\sim 4/5\varepsilon^2 + \cdots \\ b_0 &\sim 5/4 + \cdots \end{aligned}\right\} . \tag{19}$$

We can now return to the problem of solving the leading order problem. This is given by Eqs (13) and boundary conditions (14), except that now $\theta_0'(0)$ is known, via

$$\theta_0'(0) = -\lambda_c g(\varepsilon) ,$$

where $g(\varepsilon) = \exp(b_0/(1 + \varepsilon b_0))$ with b_0 as given by (18b) is known. To solve this problem we re-scale Eqs (13) by writing

$$\theta_0 = (\lambda_c g(\varepsilon))^{4/5} \bar{\theta}_0 , \qquad f_0 = (\lambda_c g(\varepsilon))^{1/5} \bar{f}_0 , \qquad \bar{y} = (\lambda_c g(\varepsilon))^{1/5} y .$$

This leaves Eqs (13) essentially unaltered except that now we have the boundary condition

$$\bar{\theta}_0'(0) = -1 \quad \text{on } \bar{y} = 0 . \tag{20a}$$

This problem has a solution which depends only upon σ with $\bar{\theta}_0(0) = c_0(\sigma)$, say. Hence

$$\theta_0(0) = (\lambda_c g(\varepsilon))^{4/5} c_0(\sigma) , \tag{20b}$$

and consequently

$$\lambda_c = \left(\frac{b_0(\varepsilon)}{c_0(\sigma)}\right)^{5/4} \Big/ g(\varepsilon) . \tag{20c}$$

Thus the problem of finding the critical points λ_c has been reduced to solving a standard free convection problem given by Eqs (13) subject to boundary condition (20a). The critical points are then calculated from (20c) using (18b).

The numerical solution of Eqs (13) subject to boundary condition (20a) for general values of σ is straightforward and the results ($\bar{\theta}_0(0)$ plotted against σ) are shown in Fig. 3. To complete the discussion of our basic problem we obtain results valid for large and small values of σ. The behaviour of the solution of Eqs (13) and (20a) for large σ follows closely that derived by Stewartson and Jones [15] and Roy [16] for similar problems. There is a thin inner region of thickness of $O(\sigma^{-1/5})$, in which we scale

$$f_0 = \sigma^{-4/5} F , \qquad \theta_0 = \sigma^{-1/5} H , \qquad \zeta = \sigma^{1/5} y , \tag{21a}$$

with Eqs (13) giving, at leading order,

$$F'''' + H = 0 , \qquad H'' + FH' = 0 , \tag{21b}$$

subject to the boundary conditions

$$F(0) = F'(0) = 0 , \qquad H'(0) = -1 , \tag{21c}$$

$$F'' \to 0 , \qquad H \to 0 \quad \text{as } \zeta \to \infty , \tag{21d}$$

(primes now denote differentiation with respect to ζ).

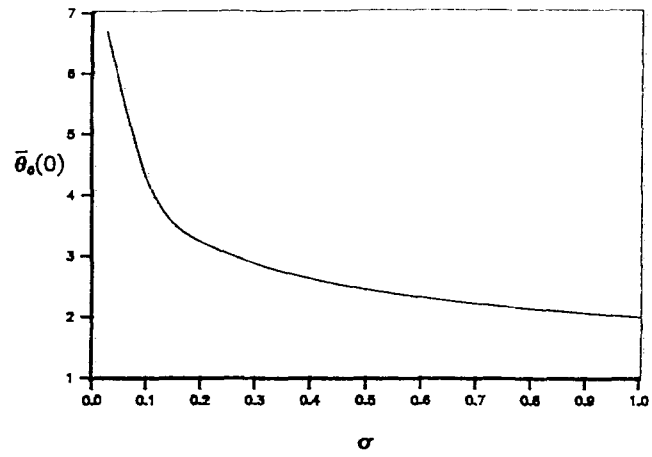

(a)

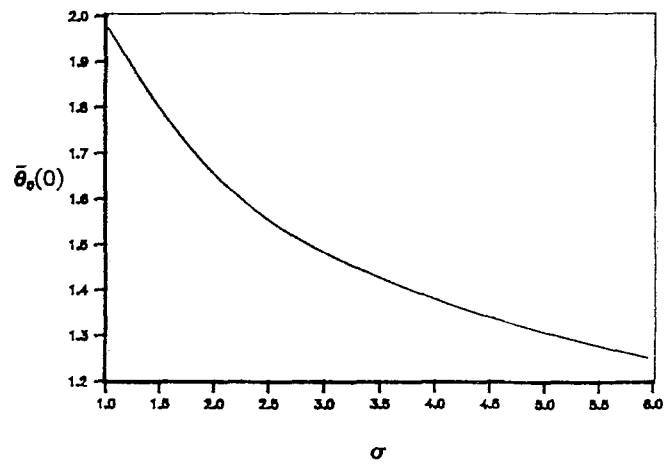

(b)

Fig. 3. Graph of $\bar{\theta}_0(0) = c_0(\sigma)$ obtained from the numerical solution of Eqs (13) subject to boundary condition (20a) for (a) $\sigma \leqslant 1$, (b) $\sigma \geqslant 1$.

The numerical solution of this leading order problem is standard, and we find that

$$H(0) = 1.63657\,, \qquad F''(0) = 1.57011\,,$$

from which it follows that

$$\bar{\theta}_0(0) = c_0(\sigma) \sim 1.63657\sigma^{-1/5} + \cdots \quad \text{as } \sigma \to \infty\,. \tag{22}$$

At the outer edge of the inner region $F \sim A_0\zeta + B_0$, for constants $A_0 = 1.13156$ and $B_0 = 0.67296$ and an outer region is required in which $\theta_0 \equiv 0$ and in which

$$f_0 = \sigma^{-3/10}\phi\,, \qquad Y = \sigma^{-3/10}y\,, \tag{23a}$$

giving the equation, at leading order

$$\phi''' + \phi\phi'' - \phi'^2 = 0\,, \tag{23b}$$

subject to

$$\phi \sim A_0 Y + \cdots \quad \text{as } Y \to 0\,, \qquad \phi' \to 0 \quad \text{as } Y \to \infty\,. \tag{23c}$$

It is readily seen that this problem has the solution

$$\phi = \sqrt{A_0}(1 - \exp(-\sqrt{A_0}Y))\,. \tag{24}$$

Finally we note that (22) implies that the critical points become large, of $O(\sigma^{1/4})$, as $\sigma \to \infty$. In particular

$$\lambda_c \sim 0.5402 \frac{b_0(\varepsilon)^{5/4}}{g(\varepsilon)} \sigma^{1/4} \quad \text{as } \sigma \to \infty\,, \tag{25a}$$

with, for example for $\varepsilon = 0$, $\lambda_c \sim 0.2045\sigma^{1/4}$.

To obtain a solution valid for σ small we follow the discussion given by Merkin [17]. Here there is an inner layer of thickness $O(\sigma^{1/10})$, in which we put

$$f_0 = \sigma^{-1/10} g\,, \qquad \theta_0 = \sigma^{-2/5} h\,, \qquad \eta = \sigma^{-1/10} y\,, \tag{26a}$$

with, at leading order,

$$h = \gamma_0^2\,, \tag{26b}$$

for some constant γ_0 to be determined. Then, from Eqs (13),

$$g''' + \gamma_0^2 + gg'' - g'^2 = 0\,. \tag{26c}$$

The details of the solution of Eq. (26c) are not important, except to note that

$$g \sim \gamma_0 \eta + \delta_0 \quad \text{as } \eta \to \infty\,, \tag{27}$$

An outer region, of thickness $O(\sigma^{-2/5})$, is then required, in which

$$f_0 = \sigma^{-3/5} G\,, \qquad \theta_0 = \sigma^{-2/5} T\,, \qquad \xi = \sigma^{2/5} y\,. \tag{28a}$$

At leading order we obtain the problem

$$GG'' - G'^2 + T = 0\,, \tag{28b}$$

$$T'' + GT' = 0\,, \tag{28c}$$

subject to

$$G' \to 0\,, \qquad T \to 0 \quad \text{as } \xi \to \infty\,, \tag{28d}$$

$$G \sim \gamma_0 \xi + \cdots\,, \qquad T \sim \gamma_0^2 + \cdots \quad \text{as } \xi \to 0\,. \tag{28e}$$

It is the numerical solution of this problem in the outer layer which determines the constant γ_0. A little care is required in doing this, as is described in [17], and we find that $\gamma_0 = 1.2149$, from which we obtain

$$\theta_0(0) = c_0(\sigma) \sim 1.4760\sigma^{-2/5} + \cdots \quad \text{as } \sigma \to 0\,, \tag{29a}$$

(29a) implies that the critical points decrease with decreasing σ, and, in particular,

$$\lambda_c \sim 0.6146\left(= 0.6146\frac{b_0(\varepsilon)^{5/4}}{g(\varepsilon)}\sigma^{1/2}\right)^{4/5} \quad \text{as } \sigma \to 0\,. \tag{29b}$$

To obtain an insight into how the critical points vary with ε, we took $\sigma = 1$, for which we find that $c_0 = 1.99627$, and hence

$$\lambda_c = 0.4214 b_0^{5/4} \exp\left(-\frac{b_0}{1+\varepsilon b_0}\right), \quad \varepsilon \leqslant 1/5\,, \tag{30a}$$

where b_0 is given by (18b). Plots of λ_c against ε are shown in Fig. 4 where the upper curve corresponds to the lower turning points and the lower curve to the upper turning point.

To complete this discussion we need to consider the behaviour of the lower and upper turning points, $\lambda_c^{(1)}$ and $\lambda_c^{(2)}$ respectively, as $\varepsilon \to 0$. Using (19), we find that, from (20c),

$$\lambda_c^{(1)} \to \left(\frac{5}{4}\right)^{5/4} \mathrm{e}^{-5/4} c_0(\sigma)^{-5/4}\,, \tag{30b}$$

$$\lambda_c^{(2)} \sim \left(\frac{4}{5\varepsilon^2}\right)^{5/4} \mathrm{e}^{-1/\varepsilon} c_0(\sigma)^{-5/4}\,, \tag{30c}$$

as $\varepsilon \to 0$. Note that for $\sigma = 1$, $\lambda_c^{(1)} \to 0.1596$ (in agreement with the results shown in Fig. 1) and that the upper turning point is at an increasingly smaller value of λ (and, from (20b), at an increasingly larger value of $\theta(0)$) as $\varepsilon \to 0$, suggesting that the upper branch of solutions correspond to very large values of surface temperature.

Finally in this section, we consider the behaviour of the bifurcation diagrams for λ small (on the lower branch) and for λ large (on the upper branch). For λ small, a consideration of Eqs (10) suggests that we put

$$f = \lambda^{1/5} F(\zeta)\,, \qquad \theta = \lambda^{4/5} h(\zeta)\,, \qquad \zeta = \lambda^{1/5} y\,, \tag{31a}$$

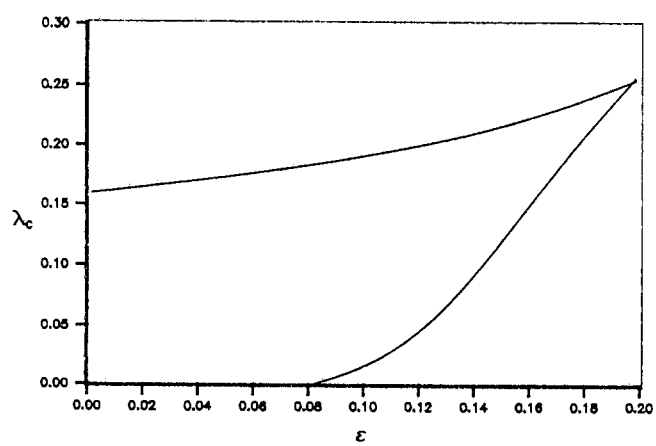

Fig. 4. Variation of the critical points λ_c with ε for $\sigma = 1$, as calculated from expressions (18b) and (30a).

(31a) shows that the boundary layer thickness becomes large, of $O(\lambda^{-1/5})$, as $\lambda \to 0$. Transformation (31a) leaves Eqs (10) essentially unaltered. However, boundary condition (11a) becomes

$$h'(0) = -\exp[\lambda^{4/5}h(0)/1 + \varepsilon\lambda^{4/5}h(0)] = -(1 + \lambda^{4/5}h(0) + \cdots)\,, \tag{31b}$$

(31b) suggests looking for a solution by expanding in powers of $\lambda^{4/5}$. The leading order terms satisfying Eqs (10) and, from (31b),

$$h'(0) = -1\,. \tag{31c}$$

This problem has already arisen in our discussion of the critical points and need not be considered further. We note that

$$\theta(0) \sim \lambda^{4/5}c_0(\sigma) \quad \text{as } \lambda \to 0\,, \tag{32}$$

where $c_0(\sigma)$ is as defined earlier.

For λ large, transformation (31a) is still the appropriate one to make, with now boundary condition (11a) written as

$$h'(0) = -\exp[h(0)/\varepsilon h(0) + \lambda^{-4/5}]\,, \tag{33a}$$

(33a) suggests looking for a solution by expanding in powers of $\lambda^{-4/5}$, the leading order terms are still given by Eqs (10), with now, to leading order

$$h'(0) = -\mathrm{e}^{-1/\varepsilon}\,. \tag{33b}$$

A rescaling,

$$F = \mathrm{e}^{1/5\varepsilon}\bar{F}\,, \qquad h = \mathrm{e}^{4/5\varepsilon}\bar{h}\,, \qquad \zeta = \mathrm{e}^{1/5\varepsilon}\bar{\zeta}\,, \tag{34a}$$

leaves Eqs (10) unaltered, but with now

$$\bar{h}'(0) = -1\,. \tag{34b}$$

Again we recover our basic problem which leads to

$$\theta(0) \sim \lambda^{4/5}\,\mathrm{e}^{4/5\varepsilon}c_0(\sigma)\,, \tag{35}$$

as $\lambda \to \infty$ on the upper solution branch.

4. Fuel consumption case, $\alpha \neq 0$

(*a*) *Numerical solutions*

Equations (8) and (9) were solved numerically for representative values of various non-dimensional parameters. We considered first the case when the Prandtl and Schmidt numbers were equal, taking $\sigma = S_c = 1$. Bifurcation diagrams (plots of $\theta(0)$ against λ) are shown in Fig. 5 for ($\varepsilon = 0.0$) and Fig. 6 (for $\varepsilon = 0.1$) for increasing values of parameter α. For the case

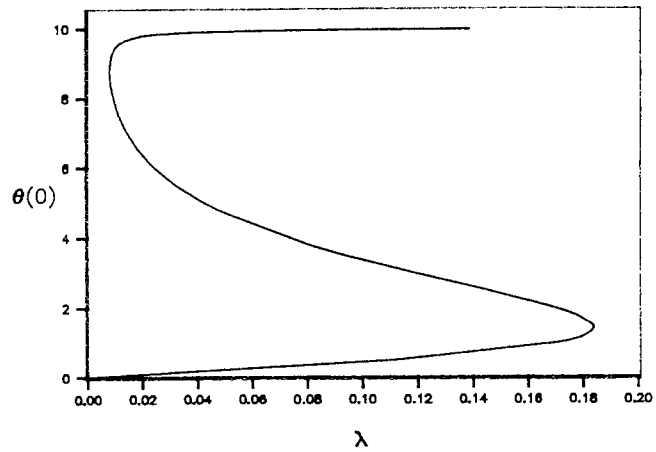

(a)

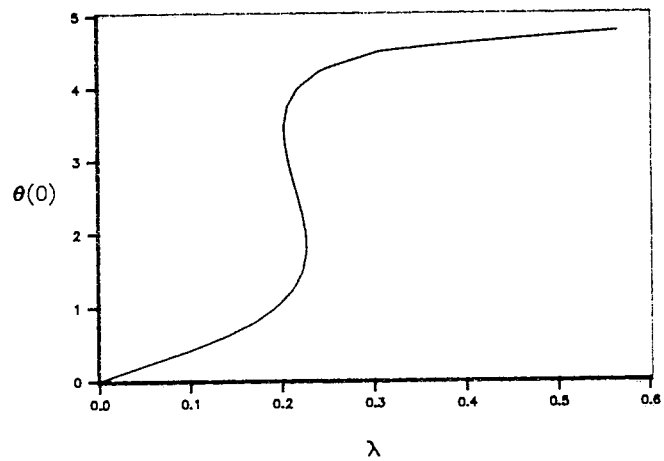

(b)

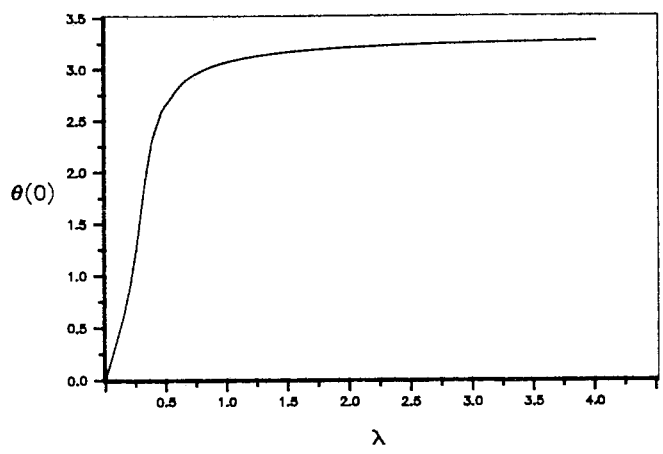

(c)

Fig. 5. Graphs of $\theta(0)$ against λ obtained from the numerical solution of Eqs (8) and (9) for $\sigma = S_c = 1.0$, $\varepsilon = 0.0$ and (a) $\alpha = 0.1$, (b) $\alpha = 0.2$, (c) $\alpha = 0.3$.

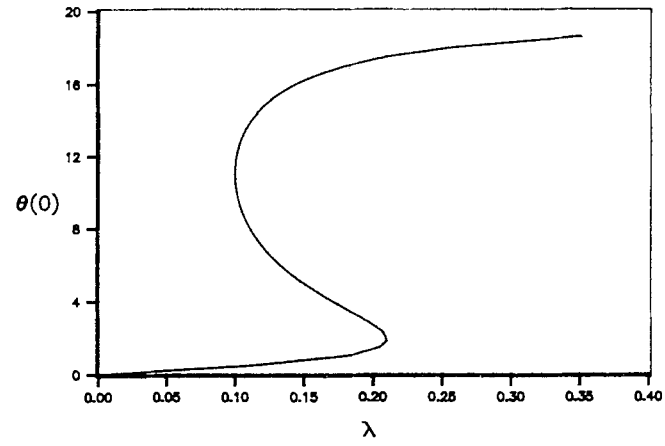

(a)

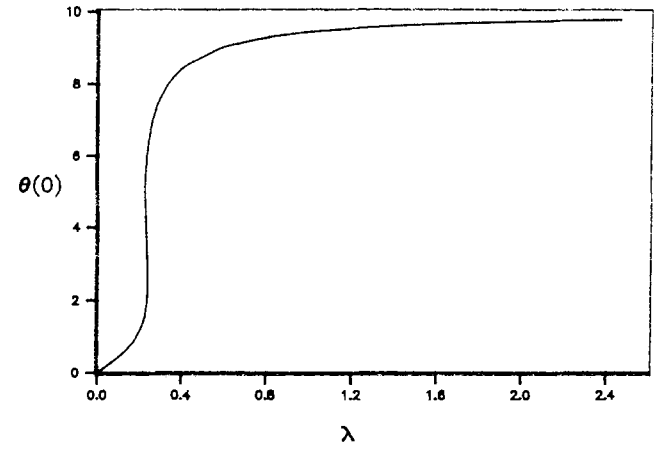

(b)

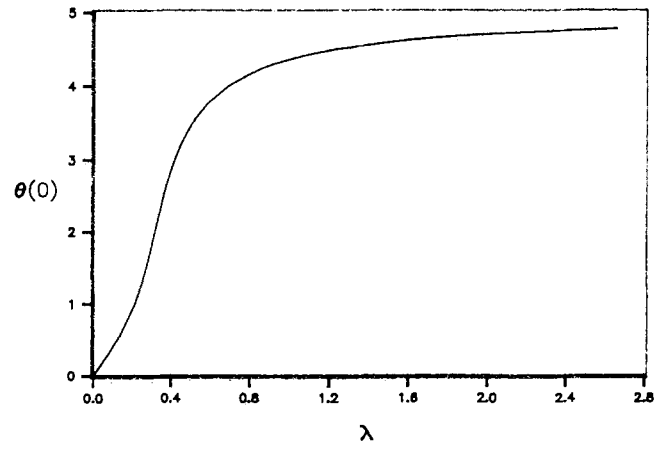

(c)

Fig. 6. Graphs of $\theta(0)$ against λ obtained from the numerical solution of Eqs (8) and (9) for $\sigma = S_c = 1.0$, $\varepsilon = 0.$ and (a) $\alpha = 0.05$, (b) $\alpha = 0.1$, (c) $\alpha = 0.2$.

$\varepsilon = 0.0$ and $\alpha = 0.1$ (Fig. 5a) we can see that there are two, well-defined turning points, at $\lambda_c^{(1)} = 0.1840$ and $\lambda_c^{(2)} = 0.0080$, respectively, and that $\theta(0) \to 1/\alpha$ as $\lambda \to \infty$ on the upper solution branch. For $\alpha = 0.2$ (Fig. 5b) there are still two turning points, but these have become much closer together, at $\lambda_c^{(1)} = 0.2270$ and $\lambda_c^{(2)} = 0.2029$. Again $\theta(0) \to 1/\alpha$ as λ increases on the upper branch. By $\alpha = 0.3$ (Fig. 5c) the curve of $\theta(0)$ against λ is monotone, showing that there is a hysteresis point in the range $0.2 < \alpha < 0.3$ for these values of ε, σ and S_c. Again $\theta(0) \to 1/\alpha$ on the upper solution branch. We tried larger values of α (not shown) and for these values the bifurcation diagrams were all monotone, suggesting that there are no further ranges of α over which multiple solutions are possible.

For $\varepsilon = 0.1$, there are still multiple solutions but these require smaller values of α. For $\alpha = 0.05$ (Fig. 6a) two turning points are clearly seen (at $\lambda_c^{(1)} = 0.2145$ and $\lambda_c^{(2)} = 0.0996$). Whereas for $\alpha = 0.1$ (Fig. 6b) these have almost merged together, here $\lambda_c^{(1)} = 0.2391$ and $\lambda_c^{(2)} = 0.2247$. By $\alpha = 0.2$ (Fig. 6c) the bifurcation diagram is monotone. Note that, as before, in all cases $\theta(0) \to 1/\alpha$ on the upper solution branch. This shows that increasing the value of ε reduces the range of over which multiple solutions are possible and suggests that for ε sufficiently large, the possibility of multiple solutions could disappear altogether. This point will be discussed later on.

We then considered the case when the values of Schmidt and Prandtl were different, taking cases when $S_c > \sigma$ and when $S_c < \sigma$. Consider the case when $\sigma = 1.0$, $S_c = 2.0$. These results are shown in Fig. 7. Again we can clearly see two turning points in bifurcation diagram when $\varepsilon = 0.0$, $\alpha = 0.2$ (at $\lambda_c^{(1)} = 0.1996$ and $\lambda_c^{(2)} = 0.0719$), which are somewhat more separated than the corresponding results for $S_c = 1.0$ (Fig. 5b). These two turning points have almost merged at a hysteresis point by $\alpha = 0.3$ (here $\lambda_c^{(1)} = 0.2405$ and $\lambda_c^{(2)} = 0.2379$) with the curve being monotone for all values of α slightly higher than this. A similar behaviour to that for equal values of σ and S_c was observed by increasing the value of ε. Here for $\varepsilon = 0.1$ a hysteresis point is suggested between $\alpha = 0.1$ and $\alpha = 0.2$ (Fig. 7c, where $\lambda_c^{(1)} = 0.2216$ and $\lambda_c^{(2)} = 0.1581$; and Fig. 7d). These results suggest that taking the ratio $S_c/\sigma > 1$, increases the range of α over which multiple solutions are possible. In all the cases shown in Fig. 7, $\theta(0)$ approached a limiting value on the upper solution branch as λ

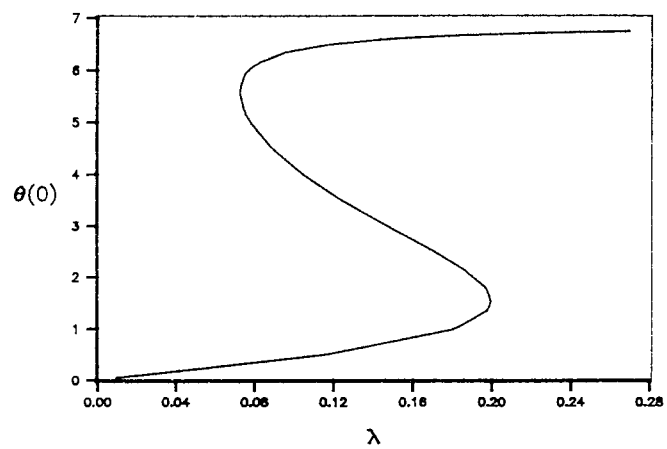

(a)

Fig. 7. Graphs of $\theta(0)$ against λ obtained from the numerical solution of Eqs (8) and (9) for $\sigma = 1.0$, $S_c = 2.0$, (a) $\varepsilon = 0.0$, $\alpha = 0.2$, (b) $\varepsilon = 0.0$, $\alpha = 0.3$, (c) $\varepsilon = 0.1$, $\alpha = 0.1$, (d) $\varepsilon = 0.1$, $\alpha = 0.2$.

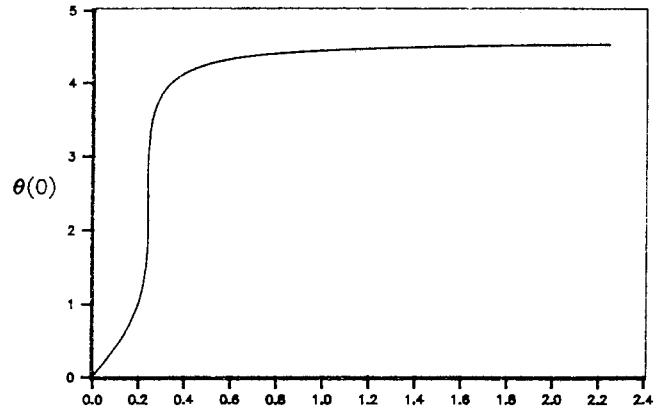

(b)

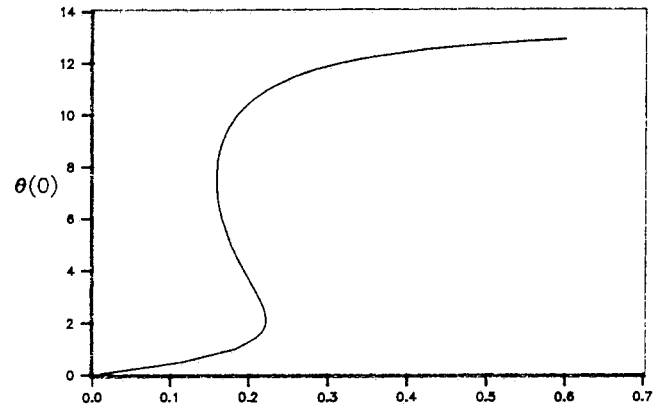

(c)

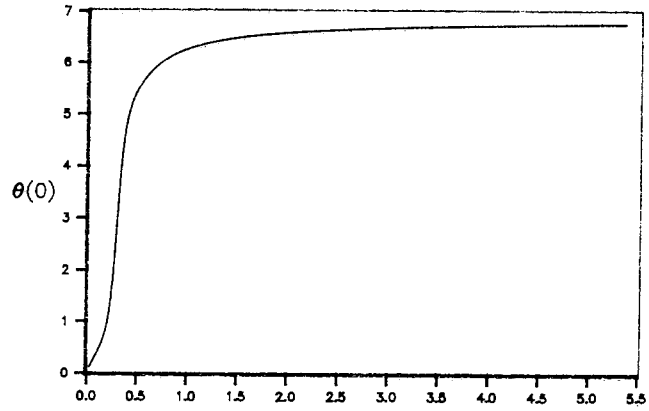

(d)

Fig. 7 (cont.).

increased. This value appeared to be independent of ε; however, there appears to be no simple correlation between this limiting value and the parameters α, S_c and σ in this case.

Finally we considered a case when $S_c < \sigma$, taking $\sigma = 1.0$ and $S_c = 0.5$. The results are shown in Fig. 8. For $\varepsilon = 0$, Figs 8a and 8b, a hysteresis point is suggested for α between $\alpha = 0.1$ and $\alpha = 0.2$. In the former case, there are two, well-defined turning points at $\lambda_c^{(1)} = 0.1993$ and $\lambda_c^{(2)} = 0.0697$, whereas in the latter case the curve is monotone. Again increasing the value of ε decreases the range of α over which multiple solutions are possible. For $\varepsilon = 0.1$ Figs 8c and 8d show that multiple solutions disappear between $\alpha = 0.05$ and $\alpha = 0.1$, with, in the former case, critical points at $\lambda_c^{(1)} = 0.2214$ and $\lambda_c^{(2)} = 0.1570$. Thus taking the ratio $S_c/\sigma < 1$ decreases the range of α over which multiple solutions are possible. Again we note that $\theta(0)$ approaches a constant value on the upper solution branch as λ is increased. This value also appears to be independent of the value of ε but appears to be different to the values approached in the $S_c/\sigma > 1$ case discussed previously.

Two important characteristics of the bifurcation diagrams in the fuel consumption ($\alpha \neq 0$) case have emerged, namely the limiting value of $\theta(0)$ on the upper solution branch and the possibility of a hysteresis point. Both of these features need further investigation. We start by considering the limiting value of $\theta(0)$.

(*b*) *Limits on the upper branch*

In the previous section we saw that $\theta(0)$ approached a limit on the upper solution branch and that this limiting value is, in general, considerably smaller than values of $\theta(0)$ on the upper branch in the non-fuel consumption case ($\alpha = 0$). This limit had an obvious value of $1/\alpha$ when $S_c = \sigma(=1.0)$. To see this, we note that in the case $S_c = \sigma$, the solution of Eq. (8c) for $a(y)$ can be written in terms of $\theta(y)$ for all values of σ as

$$a(y) = 1 - \alpha\theta(y)\,. \tag{36a}$$

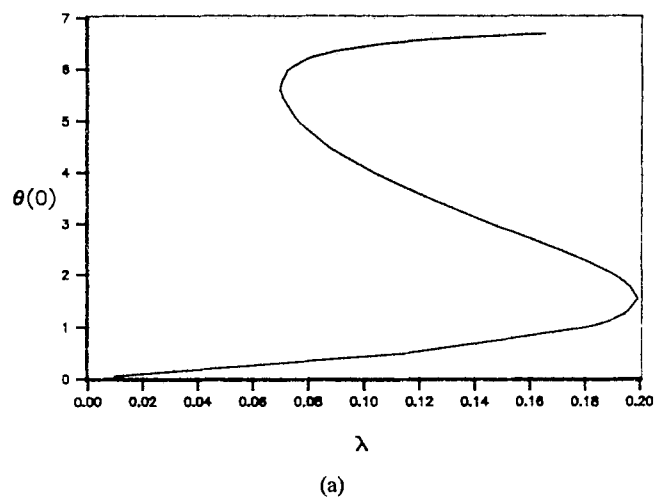

Fig. 8. Graphs of $\theta(0)$ against λ obtained from the numerical solution of Eqs (8) and (9) for $\sigma = 1.0$, $S_c = 0.5$ and (a) $\varepsilon = 0.0$, $\alpha = 0.1$, (b) $\varepsilon = 0.0$, $\alpha = 0.2$, (c) $\varepsilon = 0.1$, $\alpha = 0.05$, (d) $\varepsilon = 0.1$, $\alpha = 0.1$.

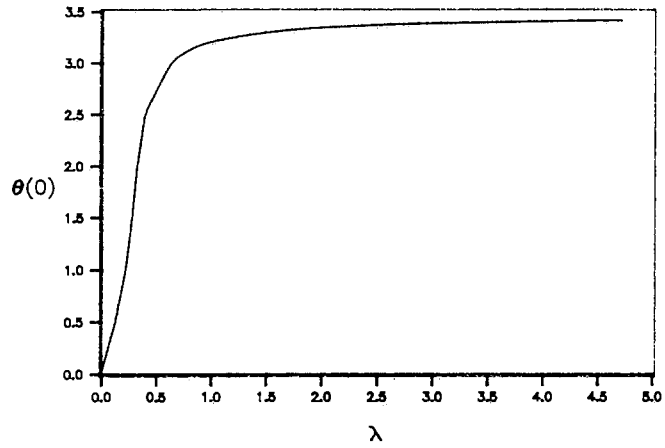

(b)

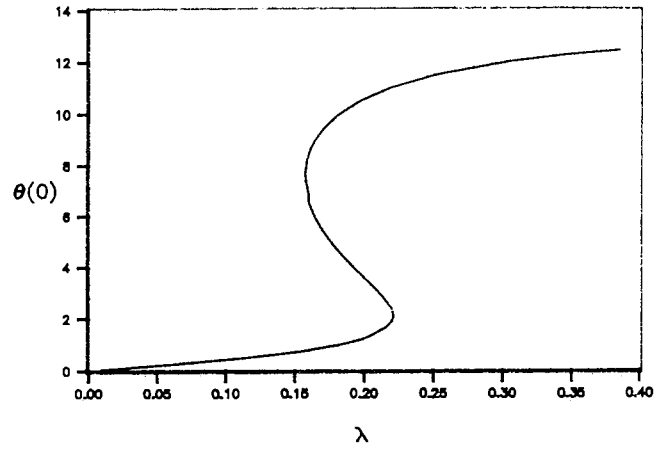

(c)

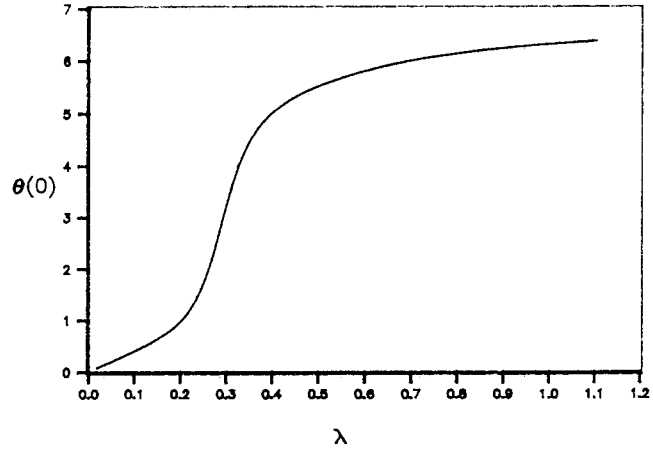

(d)

Fig. 8 (cont.).

Boundary condition (9a) then gives

$$\theta' = -\lambda(1-\alpha\theta)\exp(\theta/1+\varepsilon\theta) \quad \text{on } y=0 \tag{36b}$$

and the singularity as $\theta(0)\to 1/\alpha$ is clear.

To obtain the limiting value of $\theta(0)$ in the general case and to obtain a solution of Eqs (8) and (9) valid for λ large, we leave the equations unscaled and look for a solution by expanding

$$\begin{aligned} f(y;\lambda) &= f_0(y) + \lambda^{-1} f_1(y) + \cdots \\ \theta(y;\lambda) &= \theta_0(y) + \lambda^{-1}\theta_1(y) + \cdots \\ a(y;\lambda) &= a_0(y) + \lambda^{-1} a_1(y) + \cdots \end{aligned} \tag{37}$$

At leading order we obtain the equations

$$f_0''' + \theta_0 + f_0 f_0'' - f_0'^2 = 0\,, \tag{38a}$$

$$\frac{1}{\sigma}\theta_0'' + f_0\theta_0' = 0\,, \tag{38b}$$

$$\frac{1}{S_c} a_0'' + f_0 a_0' = 0\,, \tag{38c}$$

subject to the boundary conditions

$$f_0(0) = 0\,, \qquad f_0'(0) = 0\,, \qquad a_0(0) = 0\,, \tag{39a}$$

$$f_0' \to 0\,, \qquad \theta_0 \to 0\,, \qquad a_0 \to 1 \quad \text{as } y\to\infty\,. \tag{39b}$$

The value of θ_0 on $y=0$ is, as yet, unspecified. Hence the leading order problem contains some indeterminacy and to complete this problem we need to consider the equations for the $O(\lambda^{-1})$ terms.

At $O(\lambda^{-1})$ we obtain a system of linear equations for (f_1, θ_1, a_1) which are not important for our present discussion, and it is the boundary conditions on $y=0$ that we concentrate on, namely that

$$\left.\begin{aligned} \theta_0' &= -a_1 \exp\left(\frac{\theta_0}{1+\varepsilon\theta_0}\right) \\ a_0' &= \alpha a_1 \exp\left(\frac{\theta_0}{1+\varepsilon\theta_0}\right) \end{aligned}\right\} \quad \text{on } y=0\,. \tag{40a}$$

The consistency of Eqs (40a) then leads to the final boundary condition for leading order problem, that

$$\theta_0'(0) = -\frac{1}{\alpha} a_0'(0)\,. \tag{40b}$$

Boundary conditions (39) and (40b) are now sufficient for the solution of Eqs (38).

$\theta_0(0)$ is the limiting value on the upper solution branch, as, from (37), $\theta(0)\to\theta_0(0)$ as $\lambda\to\infty$. As can be seen from Eqs (38), (39) and (40b), this value does not involve the

activation energy parameter ε (as was noted in the numerical solutions). Also, the transformation

$$f_0 = \alpha^{-1/4}\bar{f}_0\,, \qquad \theta_0 = \alpha^{-1}\bar{\theta}_0\,, \qquad a_0 = \bar{a}_0\,, \qquad y = \alpha^{-1/4}\bar{y} \tag{41}$$

leaves Eqs (38) and boundary conditions (39) essentially unchanged (apart from derivatives now being with respect to $\bar{y}$ rather than y). Boundary condition (40b) becomes

$$\bar{\theta}_0'(0) = -\bar{a}_0'(0)\,. \tag{42}$$

Thus the leading order problem is rendered independent of the parameter α, as $\bar{\theta}_0(0)$ is dependent only on the parameters S_c and σ, with then

$$\theta_0(0) = \frac{\bar{\theta}_0(0)}{\alpha}\,. \tag{43}$$

The determination of the limiting value $\theta_0(0)$ then requires the solution of Eqs (38) subject to boundary conditions (39) and (42). For general values of S_c and σ this has to be done numerically, and results are shown in Fig. 9, where we give a plot of $\bar{\theta}_0(0)$ for varying S_c for $\sigma = 1.0$ (the case we treated in our numerical solutions). These results show that $\bar{\theta}_0(0)$ increases as S_c is increased (for a given value of σ) which is in line with our numerical solutions. Note that for the two cases we treated

$$\bar{\theta}_0(0) = 0.6925 \quad \text{for } S_c = 0.5\,, \qquad \bar{\theta}_0(0) = 1.3773 \quad \text{for } S_c = 2.0\,.$$

Finally, we note that when $S_c = \sigma$, Eqs (38) and boundary conditions (39) give $\bar{a}_0$ and $\bar{\theta}_0$ connected via

$$\bar{a}_0(y) = 1 - \frac{\bar{\theta}_0(y)}{\bar{\theta}_0(0)}\,. \tag{44}$$

This satisfies boundary condition (42) only if $\bar{\theta}_0(0) = 1$, and the simple result that $\theta(0) \to 1/\alpha$ when $S_c = \sigma$ noted above is recovered.

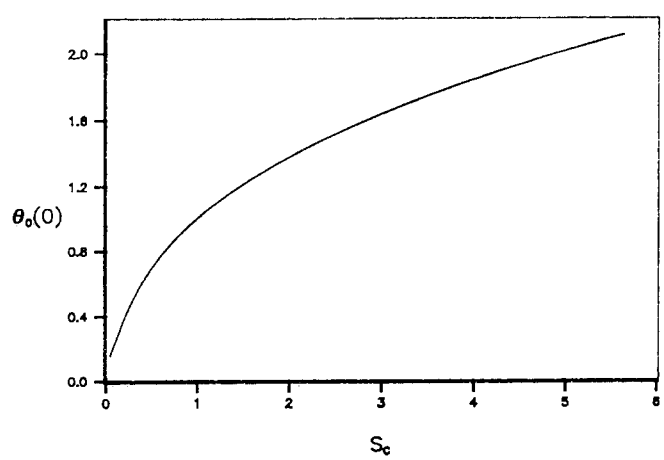

Fig. 9. Graph of $\bar{\theta}_0(0)$ plotted against S_c obtained from a numerical solution of Eqs (38), (39) and (42) for $\sigma = 1.0$.

(*c*) *Hysteresis point*

As noted previously for the case without fuel consumption, the critical points (or turning points) λ_c on the bifurcation diagrams require the solution of the leading order problem for (f_0, θ_0, a_0) (as given by Eqs (8) and (9) with $\lambda = \lambda_c$) and a non-trivial solution to linear homogeneous problem for (f_1, θ_1, a_1) obtained by making a small perturbation to this (forced by taking $\theta_1(0) = 1$, say). This leads to Eqs (15) together with the extra equation

$$\frac{1}{S_c} a_1'' + f_0 a_1' + f_1 a_0' = 0 . \tag{45a}$$

The boundary conditions are the usual homogeneous ones together with

$$\left.\begin{aligned} \theta_1' &= -\lambda_c \left[\frac{a_0 \theta_1}{(1+\varepsilon\theta_0)^2} + a_1 \right] \exp(\theta_0/(1+\varepsilon\theta_0)) \\ a_1' &= \alpha\lambda_c \left[\frac{a_0 \theta_1}{(1+\varepsilon\theta_0)^2} + a_1 \right] \exp(\theta_0/(1+\varepsilon\theta_0)) \end{aligned}\right\} \quad \text{on } y = 0 . \tag{45b}$$

As before this perturbed problem has a solution in terms of the leading order solution for all values of σ and S_c as

$$f_1 = K(yf_0' + f_0) , \qquad \theta_1 = K(y\theta_0' + 4\theta_0) , \qquad a_1 = K(ya_0' + 4a_0 - 4) , \tag{46a}$$

where, on taking $\theta_1(0) = 1$,

$$K = \frac{1}{4\theta_0(0)} . \tag{46b}$$

The substitution of (46a, b) into boundary conditions (45) then results in the single relation

$$a_0 = \frac{4(1+\varepsilon\theta_0)^2}{4\theta_0 - (1+\varepsilon\theta_0)^2} , \tag{47}$$

where in (47) a_0 and θ_0 refer to their respective values evaluated on $y = 0$.

Now we must have

$$0 \leqslant a_0(0) \leqslant 1 . \tag{48a}$$

The necessity for this condition is clear on physical grounds and also readily deduced from Eq. (8c). In fact it is clear from this equation that $a(y)$ must be monotone increasing on $0 \leqslant y \leqslant \infty$ (and from (8b) that $\theta(y)$ must be monotone decreasing on $0 \leqslant y \leqslant \infty$).

The left hand condition in (48a) implies that $\theta_0(0)$ must be in the range

$$\frac{2 - \varepsilon - 2\sqrt{1-\varepsilon}}{\varepsilon^2} < \theta_0(0) < \frac{2 - \varepsilon + 2\sqrt{1-\varepsilon}}{\varepsilon^2} . \tag{49a}$$

Equation (49a) shows that a necessary condition for the existence of critical points (and a subsequent hysteresis point) is that $\varepsilon < 1$. When $\varepsilon = 0$, condition (49a) reduces to $\theta_0(0) > 1/4$.

The right hand inequality in (48a) implies that $\theta_0(0)$ must be in the range

$$\frac{2-5\varepsilon-2\sqrt{1-5\varepsilon}}{5\varepsilon^2} \leqslant \theta_0(0) \leqslant \frac{2-5\varepsilon+2\sqrt{1-5\varepsilon}}{5\varepsilon^2}. \tag{49b}$$

Equation (49b) gives the necessary condition for existence of a hysteresis point that

$$\varepsilon \leqslant 1/5. \tag{49c}$$

For $\varepsilon > 1/5$, the bifurcation diagrams are all monotone. It can be shown that, when (49c) is satisfied, condition (49b) is a more severe restriction on $\theta_0(0)$ than condition (49a).

To proceed further, we require another relation connecting $a_0(0)$ and $\theta_0(0)$. This is not readily available for general values of the parameters and requires numerical solutions of Eqs (8). However, for the special case $S_c = \sigma$, we have the result (36a), which holds for all σ. Using this in condition (47) we can eliminate a_0 and obtain a relation connecting θ_0, α and ε at which critical points exist, namely

$$\alpha\varepsilon^2\theta_0^3 + (2\varepsilon\alpha - 4\alpha - 5\varepsilon^2)\theta_0^2 + (4 - 10\varepsilon + \alpha)\theta_0 - 5 = 0. \tag{50}$$

Equation (50) reduces to (18b), previously obtained for the case $\alpha = 0$.

For $\varepsilon = 0$, Eq. (50) becomes

$$4\alpha\theta_0^2 - (4 + \alpha)\theta_0 + 5 = 0, \tag{51a}$$

with solutions

$$\theta_0 = \frac{4 + \alpha \pm \sqrt{\alpha^2 - 72\alpha + 16}}{8\alpha}. \tag{51b}$$

Equation (51b) leads to condition that

$$\alpha \leqslant 4(9 - 4\sqrt{5}) = 0.22291 \tag{51c}$$

for the existence of multiple solutions. Hence, there is a hysteresis point in the bifurcation diagram when

$$\alpha = \alpha_H = 4(9 - 4\sqrt{5}), \qquad \varepsilon = 0. \tag{51d}$$

For $\alpha \leqslant \alpha_H$ (and $\varepsilon = 0$) there is a range of λ over which multiple solutions exist, and for $\alpha > \alpha_H$ the variation of $\theta_0(0)$ with λ is monotone increasing. The value given by (51d) is in line with point found in the numerical solutions.

For the general values of α and ε we have to solve Eq. (50) for $\theta_0(0)$, subject to the restriction $\varepsilon \leqslant 1/5$ (given by (49c)) and that $\theta_0(0) \leqslant 1/\alpha$ (implied by (36a)). It is clear that Eq. (50) has at least one positive root and it is also straightforward to show (by putting $\theta_0 = 1/\alpha$ in (50)) that this largest root does not satisfy the condition $\theta_0 < 1/\alpha$. Thus, it is the two smaller positive roots (when they exist) that are required, with the hysteresis points then arising when these two roots are co-incident. Consequently, to determine these hysteresis points we have to solve Eq. (50) simultaneously with the equation

$$3\alpha\varepsilon^2\theta_0^2 + 2(2\varepsilon\alpha - 4\alpha - 5\varepsilon^2)\theta_0 + (4 - 10\varepsilon + \alpha) = 0 \tag{52}$$

derived from it. θ_0 can be eliminated from these equations giving a relation between α and ε at which hysteresis points occur. It was found very much easier to do this numerically and a

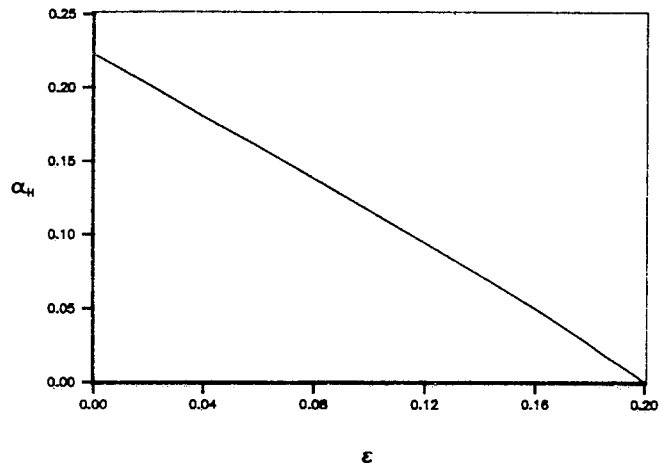

Fig. 10. Graph of hysteresis points α_H plotted against ε obtained from Eqs (50) and (52). For $\alpha < \alpha_H$ multiple solutions and for $\alpha > \alpha_H$ the bifurcation diagram is monotone.

curve of hysteresis points $\alpha_H(\varepsilon)$ plotted against ε is shown in Fig. 10. This curve divides the positive quadrant of $\varepsilon - \alpha$ plane into two regions, with qualitatively different behaviour in each region. For $\alpha < \alpha_H$ there is a range of parameter values over which multiple solution exist, while for $\alpha > \alpha_H$ the bifurcation diagram is monotone. Note that this result holds for all values of σ.

Finally, we note how the critical point λ_c can be calculated for values of $\alpha < \alpha_H(\varepsilon)$. We first solve Eq. (50) to obtain a solution $\theta_0(0) = g(\alpha, \varepsilon)$ (say) which gives, from (36a), $a_0(0) = 1 - \alpha g(\alpha, \varepsilon)$. For the case $S_c = \sigma$, we can eliminate $a_0(y)$ from the system of Eqs (38) again using (36a). Thus, we have to solve Eqs (38a, b) subject to the boundary condition

$$\theta_0'(0) = -\lambda_c(1 - \alpha g)\exp(g/1 + \varepsilon g) = -\lambda_c G(\alpha, \varepsilon)\,, \tag{53a}$$

where, since $g(\alpha, \varepsilon)$ is known, $G(\alpha, \varepsilon)$ will also be known. As before, we rescale by writing

$$f_0 = (\lambda_c G)^{1/5}\bar{f}_0\,, \qquad \theta_0 = (\lambda_c G)^{4/5}\bar{\theta}_0\,, \qquad \bar{y} = (\lambda_c G)^{1/5} y\,. \tag{53b}$$

This leaves Eqs (38a, b) essentially unaltered, with boundary condition (53a) becoming

$$\bar{\theta}_0'(0) = -1\,. \tag{53c}$$

Thus we are back to our basic problem, with $\bar{\theta}_0(0) = c_0(\sigma)$, defined earlier. The critical points are given by

$$\lambda_c = \left(\frac{g(\alpha,\varepsilon)}{c_0(\sigma)}\right)^{5/4} \frac{1}{G(\alpha, \varepsilon)}\,. \tag{53d}$$

5. Time dependent problem

There are two additional aspects of the initial-value problem (5, 7) that need to be considered, namely the stability of the stationary states discussed above the time evolution

from the initial unreacted configuration. The first of these requires considerable further discussion and this aspect will be treated in a subsequent paper. However, we can say something briefly about the development of the solution from initial conditions (5).

The initial-value problem can be solved numerically using standard finite-difference methods, and we illustrate the results with two representative examples. First, we took a no fuel consumption case, $\alpha = 0$ and $\varepsilon = 0.0$. The results are shown in Fig. 11, where we plot values of the wall temperature $\theta_0(0, t)$ against t for different values of λ. Here $\lambda_c^{(1)} = 0.1913$ and for values of $\lambda < \lambda_c^{(1)}$ the solution approaches the steady state values on the lower branch (shown in Fig. 2). For $\lambda > \lambda_c^{(1)}$ the solution becomes unbounded with a local finite-time blowup occurring. The time to reach this blowup increases as λ approaches $\lambda_c^{(1)}$ as is illustrated more clearly in Fig. 11b. This is to be expected and is in line with calculations of 'time to ignition' in other (though somewhat different) combustion problems, see, for example, Boddington et al. [18] and Gray and Merkin [19].

A similar situation arises when we allow for fuel consumption taking $\alpha \neq 0$. The results for

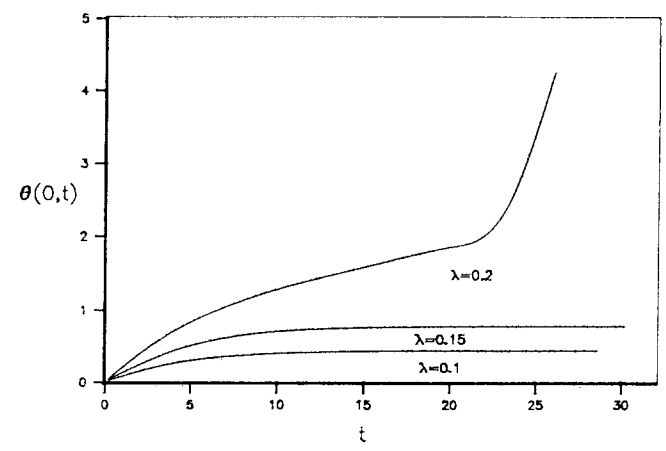

(a)

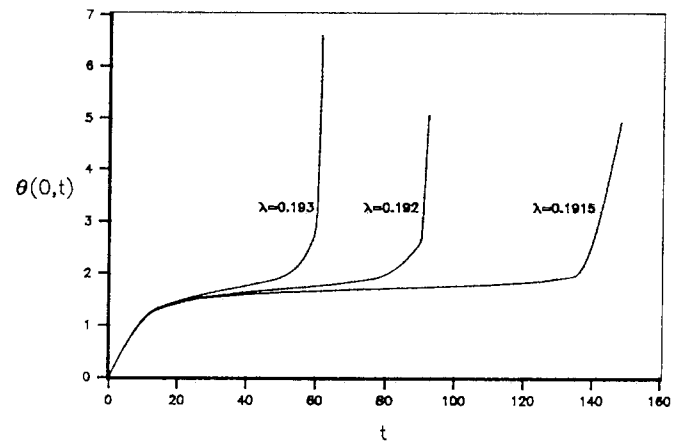

(b)

Fig. 11. Graphs of the wall temperature $\theta(0, t)$ obtained from a numerical solution of initial-value problem (5, 7) for $\varepsilon = 0.0$, $\sigma = 1.0$, $\alpha = 0.0$ for (a) $\lambda = 0.1, 0.15, 0.2$ and (b) $\lambda = 0.1915, 0.192, 0.193$. Here $\lambda_c^{(1)} = 0.1913$.

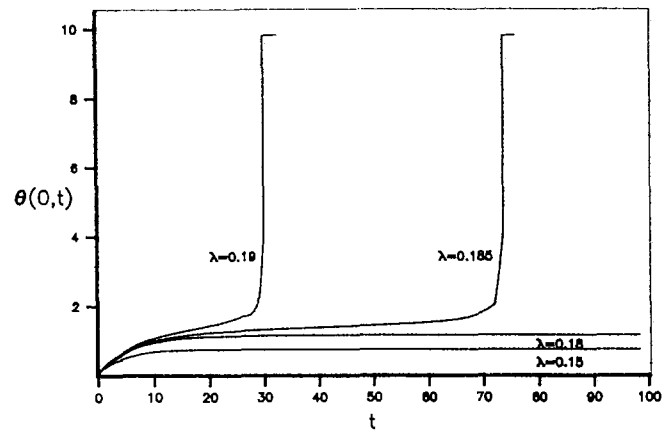

Fig. 12. Graphs of the wall temperature $\theta(0, t)$ obtained from a numerical solution of the initial-value problem (5, 7) for $\varepsilon = 0.0$, $\alpha = 0.1$, $\sigma = 1$, $S_c = 1$ and $\lambda = 0.15, 0.18, 0.185, 0.19$. Here $\lambda_c^{(1)} = 0.1837$.

$\varepsilon = 0$, $\alpha = 0.1$ ($S_c = \sigma = 1$) are shown in Fig. 12. Here $\lambda_c^{(1)} = 0.1837$ and for value of $\lambda < \lambda_c^{(1)}$ the steady state values on the lower solution branch are approached for t large. However, now there is also an upper solution branch (Fig. 5) and it is these values that are approached for $\lambda > \lambda_c^{(1)}$. The same behaviour was observed for other cases considered and not shown here.

The above suggests that both the lower and upper solution branches are stable (at least over a wide range of parameter values). We also know that the critical points correspond to a real eigenvalue changing sign (saddle-node bifurcation) and hence we expect the middle solution branch to be unstable, at least close to the critical points. Whether this middle branch is always unstable or whether there are further (Hopf) bifurcations on this branch leading to stable periodic solutions, as reported in a purely reaction-diffusion combustion problem by McGarry and Scott [20], is yet to be determined. An approximate solution, based on integrated forms of the boundary-layer equations can be constructed. This leads to a system of equations similar to the Sal'nikov scheme, discussed in detail by Kay and Scott [21, 22]. The corresponding steady states of this approximate solution have all the features of the present problem (saddle-node bifurcations and hysteresis points) as well as supercritical Hopf bifurcations, suggesting that these could also be a feature of the present initial-value problem (7). This aspect is to be treated more fully in a subsequent paper.

6. Discussion

We have considered in some detail a basic combustion model in which an exothermic reaction takes place on a catalytic surface. The heat released by this reaction sets up a free convection boundary-layer flow on the reacting surface. This flow in turn influences both the fluid temperature and reactant consumption setting up a three-way interaction between flow, heat transfer and concentration. Our model is motivated by situations where there is little or no imposed external flow but, more especially, by combustion reactions which have large activation energies and are highly exothermic.

The assumption of large activation energy means that the dimensionless parameter ε will be small and this, together with the highly exothermic nature of the reaction, leads us to

expect that the dimensionless parameter α will also be relatively small. However, the parameter λ can take all values (at least up to $O(1)$ and probably higher values). These considerations led us to treat λ as the natural bifurcation parameter and to obtain bifurcation diagrams for representative values of ε and α.

The smallness of parameters α and ε suggests that taking $\alpha = 0$ (no fuel consumption) and $\varepsilon = 0$ (exponential approximation) is a viable starting point. With this simplification we saw the existence of multiple solutions branches which are a characteristic feature of the full problem. On the lower solution branch, which corresponds to relatively low surface temperatures and thus to relatively slow rates of reaction, the solution for $\varepsilon = 0$, $\alpha = 0$ is quantitatively similar to the solution for small, but non-zero, values of these parameters. For example, the lower critical point $\lambda_c^{(1)}$ changes only slowly with ε (Fig. 4) when $\alpha = 0$, with similar behaviour being observed when $\alpha \neq 0$ (but small). Consequently, this much simplified model is useful in estimating the criticality of the system (i.e., the value of λ at which the behaviour undergoes a distinct qualitative change from a slow reaction state to a highly reactive state). However, the response of the system beyond this point (on the upper solution branch for example) is then very much dependent on the values of the parameters ε and α (as well as on the Prandtl number σ and Schmidt number S_c).

If we still retain the assumption that $\alpha = 0$ the difference between the solutions with $\varepsilon = 0$ and $\varepsilon \neq 0$ is in the existence of an upper solution branch in the latter case. This leads, for small ε, to the relatively large surface temperatures given by expression (35), and the neglect of reactant consumption is then inappropriate. With $\alpha \neq 0$ (though small), the qualitative form of the bifurcation diagram is kept, with there still being upper solution branches but these now correspond to much reduced surface temperatures. Thus the effect of the depletion of the reactant is clearly seen to limit the overall temperature attainable. This maximum temperature can be calculated explicitly when $S_c = \sigma$, i.e. when thermal conductivity and mass diffusivity are equal, as $\theta_w = 1/\alpha$. In dimensional terms this gives a maximum excess temperature (above ambient T_0) as $T_{\max} = QDa_0/k_c$ which is independent of the fluid properties. When $S_c \neq \sigma$ no such simple form for the maximum temperature was found, and it had to be determined by a numerical solution. We found that when $S_c > \sigma$, i.e. mass diffusivity is stronger than thermal conductivity, the maximum temperature was greater than $T_{\max}$. This situation is reversed when $S_c < \sigma$.

Acknowledgements

M.A. Chaudhary wishes to thank the Pakistan Government for the grant to undertake this research.

References

1. P.L. Chambre, On the ignition of a moving combustible gas stream. *J. Chemical Physics* 25 (1956) 417–421.
2. C.K. Law, On the stagnation-point ignition of a premixed combustible. *Int. J. Heat Mass Transfer* 21 (1978) 1363–1368.
3. C.M. Ablow, S. Schechter and H. Wise, Catalytic combustion in a stagnation point boundary layer. *Combustion Science and Technology* 22 (1980) 107–117.

4. C. Trevino, Gas-phase ignition of premixed fuel by catalytic bodies. *Combustion Science and Technology* 30 (1983) 213–219.
5. V. Giovangigli and S. Candel. Extinction limits of premixed flames in stagnation point flows. *Combustion Science and Technology* 48 (1986) 1–30.
6. X. Song, L.D. Schmidt and A. Aris, The ignition criteria for stagnation-point flow: Semenov–Frank–Kamanetskii or van't Hoff. *Combustion Science and Technology* 75 (1991) 311–331.
7. X. Song, W.R. Williams, L.D. Schmidt and A. Aris, Bifurcation behaviour in homogeneous-heterogeneous combustion: II Computations for stagnation-point flow. *Combustion and flame* 84 (1991) 292–311.
8. C.K. Law and G.I. Sivashinsky, Catalytic extension of extinction limits of stretched premixed flames. *Combustion Science and Technology* 29 (1982) 277–286.
9. P.A. Libby and F.A. Williams, Strained premixed laminar flames with two reaction zones. *Combustion Science and Technology* 37 (1984) 221–252.
10. C. Trevino and A.C. Fernandez-Pello, Catalytic flat plate boundary-layer ignition. *Combustion Science and Technology* 26 (1981) 245–251.
11. A. Linan and C. Trevino, Ignition and extinction of catalytic reactions on a flat plate. *Combustion Science and Technology* 38 (1984) 113–128.
12. A. Fakheri and R.O. Buckius, Transient analysis of heterogeneous and homogeneous combustion in boundary layer flow. *Combustion Science and Technology* 53 (1987) 259–275.
13. C.-H. Chen and J.S. Tien, Diffusion flame stabilization at the leading edge of a fuel plate. *Combustion Science and Technology* 50 (1986) 283–306.
14. W.R. William, M.T. Stenzel, X. Song and L.D. Schmidt, Bifurcation behaviour in homogeneous-heterogeneous combustion: I Experimental results over platinum. *Combustion and flame* 84 (1991) 277–291.
15. K. Stewartson and L.T. Jones, The heated vertical plate at high Prandtl number. *J. Aeronautical Sciences* 24 (1957) 379–380.
16. S. Roy, High Prandtl number free convection for uniform surface heat flux. *Trans. A.S.M.E.J. Heat Transfer* 95 (1973) 124–126.
17. J.H. Merkin, Free convection on a heated vertical plate: The solution for small Pradtl number. *J. Engineering Math.* 23 (1989) 273–282.
18. T. Boddinton, C. Feng, S.R. Kay and P. Gray, Thermal explosion, time to ignition and near-critical behaviour in uniform temperature systems. 4 effects of programmed ambient temperature. *J. Chem. Soc. Faraday Trans.* 81(2) (1985) 1795–1811.
19. B.F. Gray and J.H. Merkin, Thermal explosion: Escape times in the uniform temperature approximation. I Effects of parameter perturbations. *J. Chem. Soc. Faraday Trans.* 86(4) (1990) 597–601.
20. J.K. McGarry and S.K. Scott, Period doubling and chaos in a catalyst pellet. *Physics letters* A 145 (1990) 23–26.
21. P. Gray, S.R. Kay and S.K. Scott, Oscillations of an exothermic reaction in a closed system. I Approximate (exponential) representation of Arrhenius temperature dependence. *Proc. R. Soc. Lond.* A416 (1988) 321–341.
22. S.R. Kay and S.K. Scott, Oscillations of a simple exothermic reaction in a closed system. II Exact Arrhenius kinetics. *Proc. R. Soc. Lond.* A416 (1988) 343–359.